

Original article

Design, synthesis and molecular modeling study of acylated 1,2,4-triazole-3-acetates with potential anti-inflammatory activity

Ashraf M. Abdel-Megeed*, Hamdy M. Abdel-Rahman, Gamal-Eldien S. Alkaramany, Mahmoud A. El-Gendy

Medicinal Chemistry Department, Faculty of Pharmacy, Assiut University, Assiut 71526, Egypt

Received 22 January 2008; received in revised form 9 March 2008; accepted 13 March 2008

Available online 1 April 2008

Abstract

The present investigation is concerned with the synthesis of different acylated 1,2,4-triazole-3-acetates with the objective of discovering novel and potent anti-inflammatory agents. Structures of the synthesized compounds were elucidated by spectral and elemental analyses. The obtained compounds were evaluated for their anti-inflammatory activities as well as gastric ulcerogenic effects and acute toxicity. Results showed that 1-acylated-5-amino-1,2,4-triazole-3-acetates **3a–e** showed higher anti-inflammatory activity than the corresponding 5-acylamino derivatives **4a–e** in carageenan-induced rat paw edema test with low gastric ulcerogenicity compared with indomethacin. Furthermore, molecular modeling studies were performed in order to rationalize the obtained biological results.

© 2008 Elsevier Masson SAS. All rights reserved.

Keywords: Heteroarylacetic acids; 1,2,4-Triazole; Acylation; Anti-inflammatory; Docking; COX-2

1. Introduction

Non-steroidal anti-inflammatory drugs (NSAIDs), which are widely used for reducing pain and swelling associated with inflammation, represent a research area of continuous and ever-growing development. Aryl- and heteroarylacetic acids are well-established class of non-steroidal anti-inflammatory agents therapeutically useful in the treatment of acute and chronic inflammatory conditions. This class had produced many pharmacologically interesting compounds, several of which had been in clinical use, e.g., indomethacin and tolmetin, Fig. 1.

In the past few years, research for new non-steroidal anti-inflammatory agents had focused on numerous structural patterns of aryl- and heteroarylacetic acids [1–4].

Besides, studies that described simple chemical derivatization (esterification or amidation) of the carboxylic function of representative NSAIDs showed that this approach resulted not

only in the reduction of the ulcerogenic effect but also in an increased anti-inflammatory activity [5–7].

Furthermore, it had been reported that many compounds having a 1,2,4-triazole skeleton possessed significant anti-inflammatory activity [8–12].

On the basis of the abovementioned reports, the present work is concerned with the synthesis of different 1,2,4-triazolylacetic acid derivatives with the objective of discovering novel and potent anti-inflammatory agents that might be devoid of the gastrointestinal side effects.

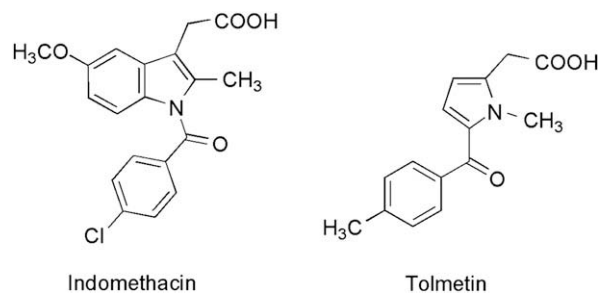
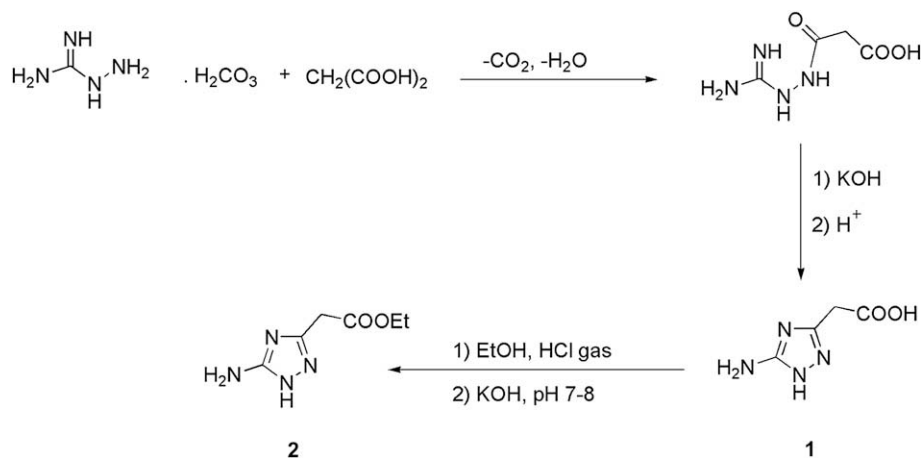


Fig. 1. Examples from heteroarylacetic acid class of NSAIDs.

* Corresponding author. Tel.: +20 101698023; fax: +20 882332776.

E-mail address: ashraf.elruby@yahoo.com (A.M. Abdel-Megeed).

Scheme 1. Synthetic pathway for intermediates **1** and **2**.

2. Results and discussion

2.1. Chemistry

Intramolecular condensation in alkaline medium of acyl derivatives of aminoguanidine is a general method used for the preparation of 3-amino-1,2,4-triazoles [13]. In the present investigation, the starting compound, 5-amino-1*H*-1,2,4-triazole-3-acetic acid **1** was prepared by gradual addition of aminoguanidine bicarbonate to a hot solution of malonic acid to give the malonylaminoguanidine followed by cyclization in alkaline medium using potassium hydroxide. Upon acidification of the formed potassium salt with concentrated hydrochloric acid to pH 4–5, the desired 5-amino-1*H*-1,2,4-triazole-3-acetic acid was obtained. Esterification of acid **1** was carried out by refluxing in ethanol saturated with hydrogen chloride gas to afford ethyl 5-amino-1*H*-1,2,4-triazole-3-acetate **2**, Scheme 1 [14].

Acylation of aminotriazoles with acid chlorides at room temperature yielded a ring-acylated product rather than the amino-acylated one [15]. Therefore, compound **2** was acylated at room temperature with different (un)substituted benzoyl chlorides in an organic aprotic solvent as dioxane, in the presence of an organic base as pyridine, to yield 1-benzoylated-1,2,4-triazole derivatives **3a–e**, Scheme 2.

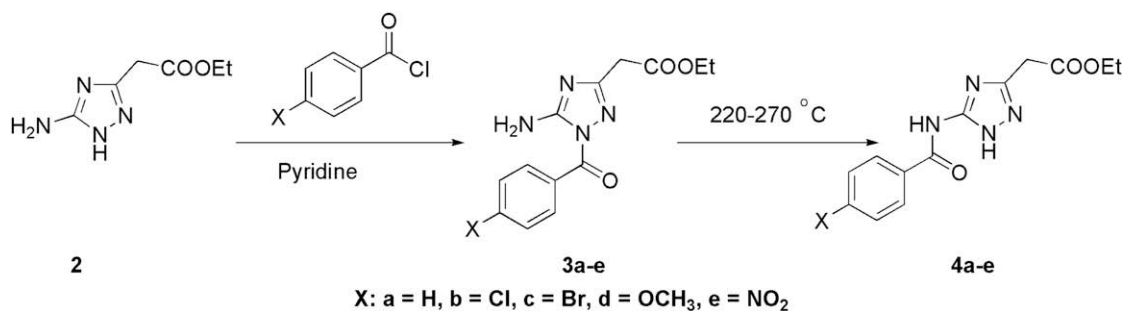
Interestingly, the 1-benzoylated-1,2,4-triazole derivatives underwent thermal rearrangement either in an organic inert

solvent, e.g., sulfolane, dimethylformamide, dimethylsulfoxide or without solvent at a temperature of 200–250 °C to give the 5-benzamido-1,2,4-triazole derivatives [15]. In the present investigation, compounds **4a–e** were synthesized in a quantitative yield by heating the corresponding 1-acyl derivatives **3a–e**, without solvent, above their melting points, Scheme 2.

Acylation of 5-amino-3-substituted-1,2,4-triazoles with acyl chlorides to yield either a ring-acylated product **A** or its 5-acylamino isomer **B** was intensively studied in the past 50 years by many authors [15–18], Fig. 2. Nevertheless, structural elucidation of the obtained compounds was in many cases ambiguous. Reiter et al. [18] reported a detailed study on the isomeric and tautomeric structures of the monoacylated 5-amino-1,2,4-triazole derivatives with the help of the spectroscopic data.

Studying the isomeric structures of type **A** and **B** monoacylated 5-amino-1,2,4-triazole derivatives with the help of their spectroscopic data resulted in the following conclusions.

In the IR spectra of the type **A** derivatives, the NH₂ bands (regardless on the type of R and R₁) appeared in the region between 3400 and 3465 cm⁻¹. On the other hand, the corresponding NH bands of the type **B** derivatives appeared as broad bands never exceeding the value of 3300 cm⁻¹ giving a good possibility for the differentiation between them. The range of the carbonyl frequencies of type **A** derivatives (1680–1700 cm⁻¹) practically overlapped the range of those

Scheme 2. Synthetic pathway for target compounds **3a–e** and **4a–e**.

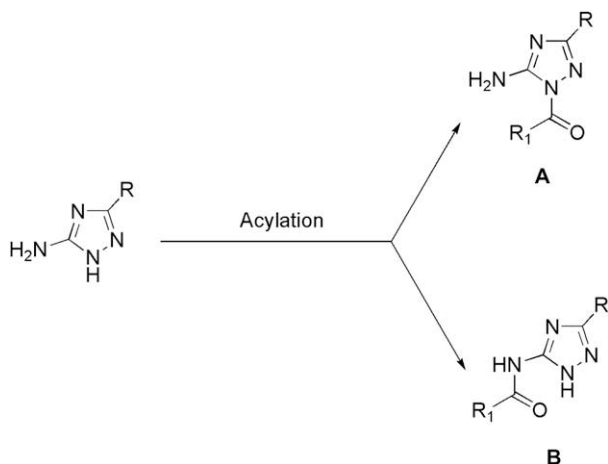


Fig. 2. Isomeric structures of monoacylated 5-amino-1,2,4-triazole derivatives.

of the corresponding type **B** derivatives ($1665\text{--}1685\text{ cm}^{-1}$). However, the carbonyl frequency of the type **A** derivatives was in all cases higher than that of the corresponding type **B** derivatives.

In the ^1H NMR spectra of type **A** derivatives, the NH_2 protons appeared as singlets between 7.8 and 8.3 ppm. On the other hand, the two broad well-separated NH signals of type **B** derivatives (NHCOR_1 and $\text{N}_1\text{--H}$) appeared between 12.3–12.8 ppm (NHCOR_1) and 13.2–14.3 ppm ($\text{N}_1\text{--H}$), respectively. This again makes it possible to differentiate between ring-acylated products **A** and their 5-acylamino isomers **B**.

2.2. Biological evaluation

The preliminary anti-inflammatory activity of the synthesized 1,2,4-triazole-3-acetic acid derivatives **1–4** was evaluated against carrageenan-induced rat paw edema using the method by Kasahara et al. [19].

Results of the anti-inflammatory activity of the tested compounds as well as indomethacin are shown in Table 1. Results showed that most of the tested compounds exhibited significant ($P < 0.05$) inhibition against carrageenan-induced rat paw edema and comparable anti-inflammatory activity relative to indomethacin. Among these derivatives, compounds **3b**, **3c** and **3e** were found to be more potent than indomethacin.

From the biological activity studies we concluded that (i) ethyl 5-amino-1*H*-1,2,4-triazole-3-acetate **2** showed higher anti-inflammatory activity than the acid derivative **1**. (ii) 1-Acylated-5-amino-1,2,4-triazole-3-acetates **3a–e** showed higher anti-inflammatory activity than the corresponding 5-acylamino derivatives **4a–e**. (iii) Among the acyl substituents in the 1-acylated and/or the 5-acylamino derivatives, the order of the anti-inflammatory activity was 4-nitrobenzoyl > 4-bromobenzoyl > 4-chlorobenzoyl > 4-methoxybenzoyl > unsubstituted benzoyl.

2.3. Gastric ulceration

Gastric ulcerogenic effects were determined in rats [20] for representative examples of the synthesized compounds, **3b** and

Table 1

Anti-inflammatory activity of 1,2,4-triazole-3-acetic acid derivatives **1–4** at 5 mg/kg dose level

Compound	Anti-inflammatory activity (5 mg/kg, oral dose) % inhibition \pm S.E.		
	1h	2h	3h
Control	0.00	0.00	0.00
Indomethacin	31.5 ± 2.32	40.1 ± 2.91	60.8 ± 3.15
1	22.3 ± 6.28	29.5 ± 6.11	48.1 ± 6.34
2	25.0 ± 4.11	33.6 ± 3.94	51.8 ± 3.93
3a	$31.6 \pm 1.54^*$	$38.5 \pm 2.54^*$	$57.5 \pm 2.90^*$
3b	$34.2 \pm 2.54^{**}$	$42.3 \pm 1.45^{**}$	$62.8 \pm 1.22^{**}$
3c	$34.8 \pm 2.87^{**}$	$43.0 \pm 2.63^{**}$	$64.1 \pm 1.45^{**}$
3d	$32.8 \pm 2.98^{**}$	$41.5 \pm 3.54^{**}$	$60.0 \pm 3.87^{**}$
3e	$36.1 \pm 1.87^{**}$	$46.3 \pm 2.45^{**}$	$68.2 \pm 2.91^{**}$
4a	$26.8 \pm 5.11^*$	$36.2 \pm 4.89^*$	$55.3 \pm 4.66^*$
4b	$31.1 \pm 3.60^*$	$39.1 \pm 3.13^*$	$58.5 \pm 2.48^*$
4c	$31.3 \pm 2.59^*$	$40.4 \pm 3.44^*$	$58.8 \pm 2.45^*$
4d	$30.2 \pm 4.11^*$	$38.2 \pm 4.60^*$	$56.0 \pm 3.85^*$
4e	$32.6 \pm 2.33^{**}$	$42.1 \pm 1.89^{**}$	$59.8 \pm 2.77^{**}$

*Significant difference at $P < 0.05$; **Significant difference at $P < 0.01$.

4b. Results indicated that compounds **3b** and **4b** did not induce any ulcerogenic effect at 10 mg/kg dose. At higher doses, the tested compounds exhibited low gastric ulcerogenicity compared with indomethacin, which caused severe ulceration at all doses, Table 2.

2.4. Acute toxicity (LD_{50})

The acute toxicity of the most active compounds; **3b**, **3c** and **3e** was determined by calculating their LD_{50} values by using graphical method [21]. The LD_{50} of compounds **3b**, **3c** and **3e** was found to be 130, 120, and 90 mg/kg, respectively, while LD_{50} of indomethacin was found to be 50 mg/kg.

2.5. Molecular modeling study

Molecular dockings as well as conformational alignment studies of compounds **3a–e** and **4a–e** were performed in order to rationalize the obtained biological results. Besides, molecular docking studies helped in understanding the various

Table 2

Ulcerogenic effects of compounds **3b** and **4b** in comparison with indomethacin

Compound	Dose mg/kg	Ratio of ulcerated animals	Ulcer index (mean \pm S.E.)
Indomethacin	10	3/6	$2.5^{**} \pm 0.18$
	50	5/6	$1.9^{**} \pm 0.15$
	100	6/6	$2.1^{**} \pm 0.17$
3b	10	0/6	0.00
	50	1/6	0.50 ± 0.1
	100	1/6	$0.75^* \pm 0.12$
4b	10	0/6	0.00
	50	0/6	0.00
	100	1/6	$0.75^* \pm 0.1$

*Significant difference at $P < 0.05$; **Significant difference at $P < 0.01$.

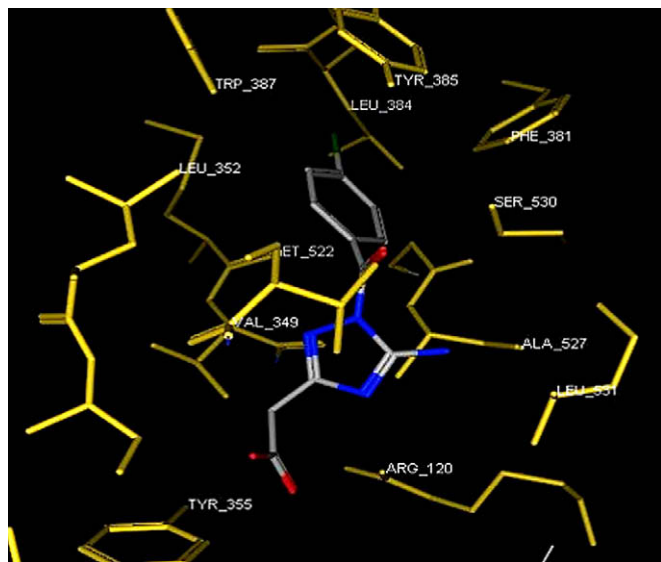


Fig. 3. Docking of the acetic acid analogue of compound **3b** (ball and stick) in the active site of murine COX-2. Hydrogen atoms of the amino acid residues have been removed to improve clarity.

interactions between the ligands and enzyme active site in detail. Since it is highly probable that the investigated compounds **3a–e** and **4a–e** undergo *in vivo* enzymatic cleavage of the ester moiety to afford the corresponding acetic acid analogues, molecular docking studies for these acetic acid derivatives were performed.

Docking studies of the inhibitors were performed by MOE (Molecular Operating Environment) [22] using murine COX-2 co-crystallized with indomethacin (PDB ID: 4COX) as a template. We performed 100 docking iterations for each ligand

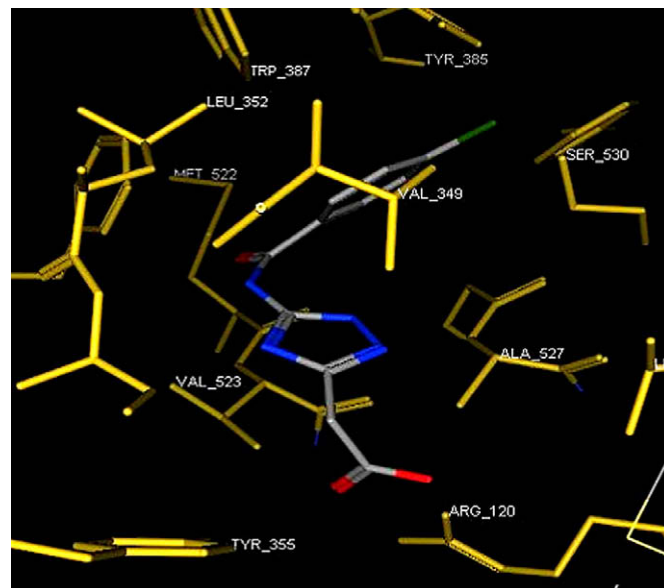


Fig. 5. Docking of the acetic acid analogue of compound **4b** (ball and stick) in the active site of murine COX-2. Hydrogen atoms of the amino acid residues have been removed to improve clarity.

and the top-scoring configuration of each of the ligand–enzyme complexes was selected on energetic grounds.

Docking of the acetic acid analogue of compound **3b**, Fig. 3, showed that the ligand was oriented so that the carboxylate moiety was in the vicinity of Arg120 residue forming an ionic interaction with the guanidinium side chain (distance = 2.45 Å). A hydrogen bond interaction between the ligand carboxylate and the OH group of Tyr355 was also observed (distance = 2.3 Å). Furthermore, the carbonyl group

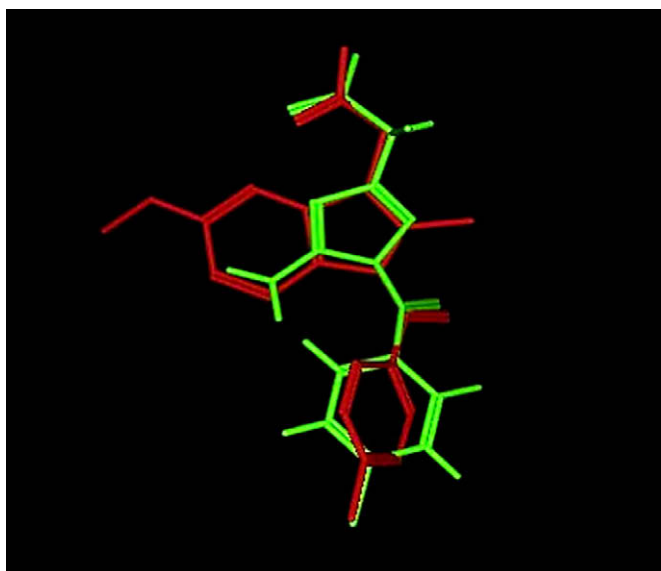


Fig. 4. Conformational alignment of indomethacin from the crystal structure of indomethacin–murine COX-2 complex (red) and that of compound **3b** acetic acid analogue from the docking simulation (green). (For interpretation of the references to colour in this figure legend, the reader is referred to the web version of this article.)

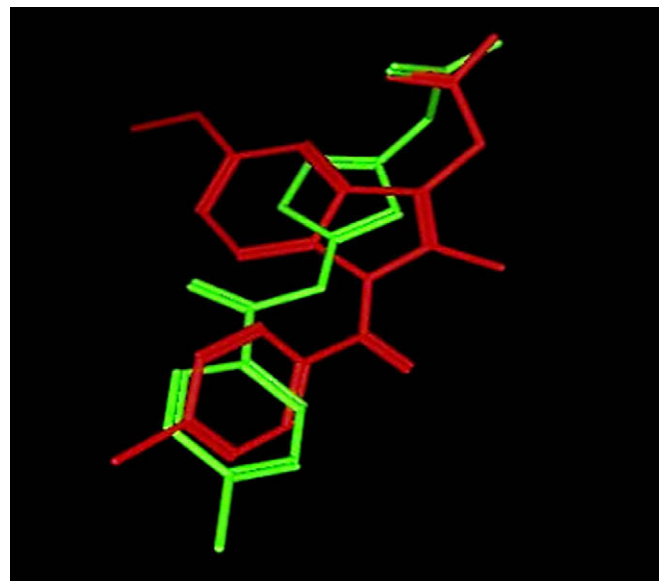


Fig. 6. Conformational alignment of indomethacin from the crystal structure of indomethacin–murine COX-2 complex (red) and that of compound **4b** acetic acid analogue from the docking simulation (green). (For interpretation of the references to colour in this figure legend, the reader is referred to the web version of this article.)

of the ligand's benzoyl moiety formed a hydrogen bond interaction with the Ser530 side chain (distance = 3.03 Å). The *p*-chlorophenyl moiety was located in the hydrophobic pocket near Tyr385 forming hydrophobic interactions with Leu352, Phe381, Leu384, Tyr385, and Trp387 residues. The 1,2,4-triazole ring is surrounded by Val349, Met522, and Ala527 residues. This arrangement is also common to all acetic acid analogues of 1-acyl-5-amino-1,2,4-triazole-3-acetates **3a–e** with small differences in contacts with the hydrophobic pocket.

Conformational superposition of indomethacin (from the X-ray crystal structure of indomethacin-COX-2 complex) and the acetic acid analogue of compound **3b** (from the docking simulation) are shown in Fig. 4. The superposition showed their hydrophilic and hydrophobic groups overlapped with each other.

From the abovementioned data, the molecular modeling studies of the examined compounds **3a,b** and their acetic acid analogues showed that they bound to the COX-2 active site with position and orientation very close to that resulting from the crystal structure of indomethacin complex with COX-2 [23]. Consequently, these observations provided a good explanation for the observed potent inhibitory activity of compounds **3a–e**.

On the other hand, docking of the acetic acid analogue of **4b** into the COX-2 active site, Fig. 5, showed almost similar contacts as observed for the corresponding 1-acyl derivative with one missing feature. Unfortunately, the interaction between the benzoyl carbonyl group of the ligand and the Ser530 side chain was lost. Accordingly, the parent triazole ring was oriented so that the carboxylate moiety was positioned near the mouth of COX-2 active site forming ionic bond with the guanidino group of Arg120 (distance = 2.51 Å). The *p*-chlorophenyl moiety was located in the vicinity of the aromatic pocket forming hydrophobic interactions with Val349, Leu352, Phe381, Tyr385, Trp387, Phe518, and Met522. This arrangement is also common to all acetic acid analogues of 5-acylamino-1,2,4-triazole-3-acetates **4a–e** with small differences in contacts with the hydrophobic pocket.

The conformational superposition of indomethacin (from the X-ray crystal structure of indomethacin-COX-2 complex) and the acetic acid analogue of compound **4b** (from the docking simulation) are shown in Fig. 6.

3. Conclusion

We reported here the synthesis of different acylated 1,2,4-triazole-3-acetates. The synthesized compounds were tested for their anti-inflammatory activity. Results showed that the most tested compounds exhibited significant anti-inflammatory activity in the carageenan-induced rat paw edema test with low gastric ulcerogenicity compared with indomethacin. Furthermore, the molecular modeling studies suggested that the 1-acyl-5-amino-1,2,4-triazole derivatives **3a–e** exhibited higher affinity for the COX-2 active site and hence increased anti-inflammatory activity than the corresponding 5-acylamino-1,2,4-triazole derivatives **4a–e**.

4. Experimental

4.1. Chemistry

Melting points were determined using an electrothermal apparatus (Stuart Scientific, England) and were uncorrected. IR spectra were recorded as KBr disk using Shimadzu IR 200-91527 spectrophotometer (Shimadzu Corp., Kyoto, Japan) and the data are given in ν_{\max} (cm^{-1}). ^1H NMR (60 MHz) spectra were carried out on Varian EM-360L, 60 MHz, (Varian, Palo Alto, CA, USA) using DMSO- d_6 as a solvent and the chemical shifts are given in δ (ppm). All NH and NH₂ protons were exchangeable with D₂O. Mass spectra were performed on Joel, JMS-600 spectrometer at an ionization voltage of 70 eV (Joel, Tokyo, Japan). Elemental analyses were performed on “Analytischer Funktionstest vario EL Fab.-Nr. 11982027” (Germany). Analyses indicated by the symbols of the elements functions were within $\pm 0.4\%$ of the theoretical values. All reactions were monitored by thin-layer chromatography (TLC) using silica gel 60 GF₂₄₅ precoated sheets 20 × 20 cm, layer thickness 0.2 mm (E-Merck, Germany) and were visualized by UV-lamp at wave length (λ) 254 nm. All chemicals and solvents were of reagent grade and the latter were distilled and dried before use.

4.1.1. Synthesis of 5-amino-1H-1,2,4-triazole-3-acetic acid (**1**) [14]

Aminoguanidine bicarbonate (13.6 g, 0.1 mol) was added gradually with stirring to a hot solution (60–70 °C) of malonic acid (10.4 g, 0.1 mol) in water (30 mL). The mixture was heated on a boiling water bath for 4 h and cooled to room temperature. Potassium hydroxide (10 g) was then added in portions and the mixture was heated to 100 °C for 2 h. The mixture was then cooled and acidified with concentrated hydrochloric acid to pH 3–4. The precipitated product was filtered off and crystallized from hot water to yield 9.3 g (65%), mp 190–192 °C (as reported) [14].

4.1.2. Synthesis of ethyl 5-amino-1H-1,2,4-triazole-3-acetate (**2**) [14]

A suspension of compound **1** (4.0 g, 0.028 mol) in ethanol (50 mL) saturated with hydrogen chloride gas was refluxed for 4 h. The reaction mixture was cooled to room temperature and adjusted to pH 7–8 with potassium hydroxide solution (20% w/v). The solvent was evaporated under reduced pressure and the residue was crystallized from hot water. Yield 64%, mp 160–162 °C. IR (KBr, cm^{-1}): 3425–3255 (NH₂, NH), 1719 (C=O), 1654, 1611 (C=N), and 1199 (C–O–C). ^1H NMR (60 MHz, DMSO- d_6 , δ ppm): 1.1 (t, 3H, CH₂CH₃); 3.6 (s, 2H, CH₂CO); 4.2 (q, 2H, CH₂CH₃); 6.2 (s, 2H, NH₂ exchangeable); 12.2 (br s, 1H, N₁–H exchangeable).

4.1.3. General procedure for the synthesis of ethyl 5-amino-1-(un)substituted benzoyl-1H-1,2,4-triazole-3-acetate (**3a–e**)

A solution of the (un)substituted benzoyl chloride (0.01 mol) in dioxane (5 mL) was added dropwise to a mixture of compound **2** (1.7 g, 0.01 mol), pyridine (1.2 mL, 0.015 mol)

and dioxane (10 mL) with constant stirring at 0–5 °C. The reaction mixture was stirred for 30 min at this temperature, then for 4 h at room temperature. The mixture was then poured onto water (50 mL) and the formed precipitate was filtered, washed with water and crystallized from methanol.

4.1.3.1. Ethyl 1-benzoyl-5-amino-1H-1,2,4-triazole-3-acetate (3a). Yield 69%; mp 126–128 °C. IR (KBr, cm^{-1}): 3415 (NH_2), 1734, 1691 ($\text{C}=\text{O}$ ester, $\text{C}=\text{O}$ amide). ^1H NMR (60 MHz, $\text{DMSO-}d_6$, δ ppm): 1.1 (t, 3H, CH_2CH_3); 3.6 (s, 2H, CH_2CO); 4.2 (q, 2H, CH_2CH_3); 7.9 (s, 2H, NH_2 exchangeable); 8.3 (m, 5H, Ar-H). Anal. ($\text{C}_{13}\text{H}_{14}\text{N}_4\text{O}_3$) C, H, N.

4.1.3.2. Ethyl 1-(4-chlorobenzoyl)-5-amino-1H-1,2,4-triazole-3-acetate (3b). Yield 75%; mp 164–165 °C. IR (KBr, cm^{-1}): 3415 (NH_2), 1731, 1684 ($\text{C}=\text{O}$ ester, $\text{C}=\text{O}$ amide). ^1H NMR (60 MHz, $\text{DMSO-}d_6$, δ ppm): 1.2 (t, 3H, CH_2CH_3); 3.6 (s, 2H, CH_2CO); 4.1 (q, 2H, CH_2CH_3); 7.6 (d, 2H, Ar-H); 7.8 (s, 2H, NH_2 exchangeable); 8.0 (d, 2H, Ar-H). MS (EI): m/z 308 [11%, M^+], m/z 310 [3.7%, $\text{M} + 2$]. Anal. ($\text{C}_{13}\text{H}_{13}\text{ClN}_4\text{O}_3$) C, H, N.

4.1.3.3. Ethyl 1-(4-bromobenzoyl)-5-amino-1H-1,2,4-triazole-3-acetate (3c). Yield 71%; mp 165–167 °C. IR (KBr, cm^{-1}): 3400 (NH_2), 1724, 1680 ($\text{C}=\text{O}$ ester, $\text{C}=\text{O}$ amide). ^1H NMR (60 MHz, $\text{DMSO-}d_6$, δ ppm): 1.1 (t, 3H, CH_2CH_3); 3.6 (s, 2H, CH_2CO); 4.2 (q, 2H, CH_2CH_3); 8.1 (d, 2H, Ar-H); 8.2 (s, 2H, NH_2 exchangeable); 8.5 (d, 2H, Ar-H). Anal. ($\text{C}_{13}\text{H}_{13}\text{BrN}_4\text{O}_3$) C, H, N.

4.1.3.4. Ethyl 1-(4-methoxybenzoyl)-5-amino-1H-1,2,4-triazole-3-acetate (3d). Yield 66%; mp 137–139 °C. IR (KBr, cm^{-1}): 3465 (NH_2), 1733, 1684 ($\text{C}=\text{O}$ ester, $\text{C}=\text{O}$ amide). ^1H NMR (60 MHz, $\text{DMSO-}d_6$, δ ppm): 1.1 (t, 3H, CH_2CH_3); 3.7 (s, 2H, CH_2CO); 4.0 (s, 3H, OCH_3); 4.2 (q, 2H, CH_2CH_3); 7.4 (d, 2H, Ar-H); 8.2 (s, 2H, NH_2 exchangeable); 8.7 (d, 2H, Ar-H). Anal. ($\text{C}_{14}\text{H}_{16}\text{N}_4\text{O}_4$) C, H, N.

4.1.3.5. Ethyl 1-(4-nitrobenzoyl)-5-amino-1H-1,2,4-triazole-3-acetate (3e). Yield 63%; mp 263–265 °C. IR (KBr, cm^{-1}): 3400 (NH_2), 1729, 1690 ($\text{C}=\text{O}$ ester, $\text{C}=\text{O}$ amide). ^1H NMR (60 MHz, $\text{DMSO-}d_6$, δ ppm): 1.2 (t, 3H, CH_2CH_3); 3.7 (s, 2H, CH_2CO); 4.3 (q, 2H, CH_2CH_3); 8.3 (s, 2H, NH_2 exchangeable); 8.8 (m, 4H, Ar-H). Anal. ($\text{C}_{13}\text{H}_{13}\text{N}_5\text{O}_5$) C, H, N.

4.1.4. General procedure for the synthesis of ethyl 5-(un)substituted benzamido-1H-1,2,4-triazole-3-acetate (4a–e)

The appropriate ethyl 1-acyl-5-amino-1,2,4-triazole-3-acetate **3a–e** (0.01 mol) was heated above the melting points (at 220–270 °C) for 10 min without solvent. After cooling, the product obtained was collected and crystallized from dioxane.

4.1.4.1. Ethyl 5-benzamido-1H-1,2,4-triazole-3-acetate (4a). Yield 95%; mp 256–258 °C. IR (KBr, cm^{-1}): 3235, 3110 (NH), 1735, 1673 ($\text{C}=\text{O}$ ester, $\text{C}=\text{O}$ amide). ^1H NMR (60 MHz, $\text{DMSO-}d_6$, δ ppm): 1.1 (t, 3H, CH_2CH_3); 3.8 (s, 2H, CH_2CO); 4.2 (q, 2H, CH_2CH_3); 7.3 (m, 5H, Ar-H); 12.8

(br s, 1H, NHCO exchangeable); 14.3 (br s, 1H, $\text{N}_1\text{–H}$ exchangeable). Anal. ($\text{C}_{13}\text{H}_{14}\text{N}_4\text{O}_3$) C, H, N.

4.1.4.2. Ethyl 5-(4-chlorobenzamido)-1H-1,2,4-triazole-3-acetate (4b). Yield 96%; mp 273–275 °C. IR (KBr, cm^{-1}): 3290, 3150 (NH), 1732, 1677 ($\text{C}=\text{O}$ ester, $\text{C}=\text{O}$ amide). ^1H NMR (60 MHz, $\text{DMSO-}d_6$, δ ppm): 1.1 (t, 3H, CH_2CH_3); 3.8 (s, 2H, CH_2CO); 4.3 (q, 2H, CH_2CH_3); 7.9 (d, 2H, Ar-H); 8.4 (d, 2H, Ar-H); 12.5 (br s, 1H, NHCO exchangeable); 13.7 (br s, 1H, $\text{N}_1\text{–H}$ exchangeable). MS (EI): m/z 308 [3%, M^+], m/z 310 [1.1%, $\text{M} + 2$]. Anal. ($\text{C}_{13}\text{H}_{13}\text{ClN}_4\text{O}_3$) C, H, N.

4.1.4.3. Ethyl 5-(4-bromobenzamido)-1H-1,2,4-triazole-3-acetate (4c). Yield 96%; mp 270–272 °C. IR (KBr, cm^{-1}): 3270, 3075 (NH), 1728, 1669 ($\text{C}=\text{O}$ ester, $\text{C}=\text{O}$ amide). ^1H NMR (60 MHz, $\text{DMSO-}d_6$, δ ppm): 1.2 (t, 3H, CH_2CH_3); 3.8 (s, 2H, CH_2CO); 4.3 (q, 2H, CH_2CH_3); 8.1 (d, 2H, Ar-H); 8.5 (d, 2H, Ar-H); 12.4 (br s, 1H, NHCO exchangeable); 13.2 (br s, 1H, $\text{N}_1\text{–H}$ exchangeable). Anal. ($\text{C}_{13}\text{H}_{13}\text{BrN}_4\text{O}_3$) C, H, N.

4.1.4.4. Ethyl 5-(4-methoxybenzamido)-1H-1,2,4-triazole-3-acetate (4d). Yield 95%; mp 256–258 °C. IR (KBr, cm^{-1}): 3275, 3120 (NH), 1733, 1672 ($\text{C}=\text{O}$ ester, $\text{C}=\text{O}$ amide). ^1H NMR (60 MHz, $\text{DMSO-}d_6$, δ ppm): 1.1 (t, 3H, CH_2CH_3); 3.8 (s, 2H, CH_2CO); 4.0 (s, 3H, OCH_3); 4.2 (q, 2H, CH_2CH_3); 7.3 (d, 2H, Ar-H); 8.2 (d, 2H, Ar-H); 12.6 (br s, 1H, NHCO exchangeable); 14.3 (br s, 1H, $\text{N}_1\text{–H}$ exchangeable). Anal. ($\text{C}_{14}\text{H}_{16}\text{N}_4\text{O}_4$) C, H, N.

4.1.4.5. Ethyl 5-(4-nitrobenzamido)-1H-1,2,4-triazole-3-acetate (4e). Yield 92%; mp > 300 °C. IR (KBr, cm^{-1}): 3190, 3090 (NH), 1728, 1670 ($\text{C}=\text{O}$ ester, $\text{C}=\text{O}$ amide). ^1H NMR (60 MHz, $\text{DMSO-}d_6$, δ ppm): 1.2 (t, 3H, CH_2CH_3); 3.7 (s, 2H, CH_2CO); 4.3 (q, 2H, CH_2CH_3); 8.8 (m, 4H, Ar-H); 12.4 (br s, 1H, NHCO exchangeable); 13.2 (br s, 1H, $\text{N}_1\text{–H}$ exchangeable). Anal. ($\text{C}_{13}\text{H}_{13}\text{N}_5\text{O}_5$) C, H, N.

4.2. Anti-inflammatory activity

Adult male albino rats of average weight (100 g \pm 10%) were divided into groups, each of six rats. Each group was treated with a suspension of the tested compound or the reference drug orally by gastric tubes at dose level of 5 mg/kg. The control animal group, on the other hand, was treated with the vehicle, CMC. After 30 min, 0.1 mL of freshly prepared carrageenan solution (1% in normal saline) was injected into the subplanar region of the right hind paw of each rat. The thickness of rat paw was measured at different time intervals (60, 120, 180 min) after administration of the test samples. The difference between the thicknesses of two paws (right and left) was taken as a measure of edema.

4.3. Gastric ulcerogenic effect

Adult male albino rats (120–200 g) were divided into groups; each of six animals. Animals were starved for 24 h

before the experiment but had free access to water. The animals were then treated orally by means of a stomach tube with suspensions of the tested compounds and the reference drug in aqueous solution of carboxymethyl cellulose, CMC, (0.5% w/v) at dose levels of 10, 50, 100 mg/kg. Control animals were treated with an equal volume of 0.5% carboxymethyl cellulose. After 6 h, the rats were sacrificed and the stomachs were removed, dissected along the greater curvature and washed with water. The lesions in gastric mucosa were determined by using stereoscopic microscope. Ulcer was defined as at least one lesion that was 0.5 mm or more in length. Lesion size (mm) was measured along its greatest length and in the case of patches; five such lesions were considered the equivalent of a 1 mm ulcer. The sum of the lesions' lengths in each group of animals was divided by their number and expressed as the gastric ulcer index.

4.4. Acute toxicity (LD_{50})

Groups of adult male albino mice, each of five animals (25–30 g) were injected intraperitoneally with graded doses of the tested compounds and the reference drug. The percentage of mortality, in each group of animals, was determined 24 h after the injection. Calculation of the LD_{50} was processed by graphical method [21].

4.5. Molecular docking

All the molecular modeling studies were carried out on an Intel Pentium 1.6 GHz processor, 512 MB memory with Windows XP operating system using Molecular Operating Environment (MOE 2005.06; Chemical Computing Group, Canada) [22] as the computational software. All the minimizations were performed with MOE until a RMSD gradient of $0.05 \text{ Kcal mol}^{-1} \text{ \AA}^{-1}$ with MMFF94X force-field and the partial charges were automatically calculated.

The X-ray crystallographic structure of murine COX-2 complexed with indomethacin (PDB ID: 4COX) was obtained from the protein data bank. The enzyme was prepared for docking studies where: (i) ligand molecule was removed from the enzyme active site. (ii) Hydrogen atoms were added to the structure with their standard geometry. (iii) MOE Alpha Site Finder was used for the active sites search in the enzyme structure and dummy atoms were created from the obtained

alpha spheres. (iv) The obtained model was then used in predicting the ligand–enzyme interactions at the active site.

References

- [1] S.S. Bahekar, D.B. Shinde, *Bioorg. Med. Chem. Lett.* 14 (2004) 1733–1736.
- [2] G. Caliendo, G. Cirino, G. Greco, E. Novellino, E. Perissutti, A. Pinto, V. Santagada, C. Silipo, L. Sorrentino, *Eur. J. Med. Chem.* 29 (1994) 381–388.
- [3] E.E. Knaus, P. Kumar, *Eur. J. Med. Chem.* 28 (1993) 881–885.
- [4] G. Daidone, B. Maggio, S. Plescia, D. Raffa, D. Schillaci, O. Migliara, A. Caruso, V.M.C. Cutuli, M. Amico-Roxas, *Il Farmaco* 53 (1998) 350–356.
- [5] S. Kalgutkar, A.B. Marnett, B.C. Crews, R.P. Rimmel, L.J. Marnett, *J. Med. Chem.* 43 (2000) 2860–2870.
- [6] G. Dannhardt, S. Laufer, *Curr. Med. Chem.* 7 (2000) 1101–1112.
- [7] D. Galanakis, A.P. Kourounakis, K.C. Tsiakitzis, C. Doulgeris, E.A. Rezza, A. Gavalas, C. Kravaritou, C. Charitos, P.N. Kourounakis, *Bioorg. Med. Chem. Lett.* 14 (2004) 3639–3643.
- [8] K. Sung, A.R. Lee, *J. Heterocycl. Chem.* 29 (1992) 1101–1109.
- [9] M.D. Mullican, M.W. Wilson, D.T. Connor, C.R. Kostlan, D.J. Schrier, R.D. Dyer, *J. Med. Chem.* 36 (1993) 1090–1099.
- [10] D.H. Boschelli, D.T. Connor, D.A. Bornemeier, R.D. Dyer, J.A. Kennedy, P.J. Kuipers, G.C. Okonko, D.J. Schrier, C.D. Wright, *J. Med. Chem.* 36 (1993) 1802–1810.
- [11] L. Czollner, G. Szilagyi, J. Lango, J. Janaky, *Arch. Pharm. (Weinheim)* 323 (1990) 225–227.
- [12] E. Palaska, G. Sahin, P. Kelicen, N.T. Durlu, G. Altinok, *Il Farmaco* 57 (2002) 101–107.
- [13] J.H. Boyer, in: R.C. Elderfield (Ed.), *Heterocyclic Compounds*, Wiley-VCH, New York, USA, 1961, pp. 425–460.
- [14] T.P. Kofman, T.A. Uvarova, G.Y. Kartseva, *Russ. J. Org. Chem.* 31 (1995) 240–244.
- [15] N.P. Peet, L.E. Baugh, S. Sunder, J.E. Lewis, E.H. Matthews, E.L. Olberding, D.N. Shah, *J. Med. Chem.* 29 (1986) 2403–2409.
- [16] A. Dzygiel, B. Rzeszotarska, E. Masiukiewicz, P. Cmoch, B. Kamiński, *Chem. Pharm. Bull.* 52 (2004) 192–198.
- [17] Z.N. Fidler, E.F. Shibanova, P.V. Makerov, I.D. Kalikhman, A.M. Shulunova, G.I. Sarapulova, L.V. Klyba, V.Y. Vitkovskii, N.N. Chipanina, V.A. Lopyrev, M.G. Voronkov, *Chem. Heterocycl. Compd.* 16 (1980) 1079–1083.
- [18] J. Reiter, L. Pongo, P. Dvortsak, *J. Heterocycl. Chem.* 24 (1987) 127–142.
- [19] Y. Kasahara, H. Hikino, S. Tsurufuji, M. Watanabe, K. Ohuhi, *Planta Med.* 51 (1985) 325–331.
- [20] H. Ikuta, H. Shirota, S. Kobayashi, Y. Yamagishi, K. Yamada, I. Yamatsu, K. Katayama, *J. Med. Chem.* 30 (1987) 1995–1998.
- [21] A.A. Bekhit, H.T. Fahmy, *Arch. Pharm. Pharm. Med. Chem.* 336 (2003) 111–118.
- [22] Molecular Operating Environment (MOE), Version 2005.06, Chemical Computing Group, Inc., Montreal, Quebec, Canada, 2005. <<http://www.chemcomp.com>>.
- [23] R. Pouplana, J.J. Lozano, J. Ruiz, *J. Mol. Graphics Model.* 20 (2002) 329–343.